

130 mA/mm β -Ga₂O₃ MESFET with Low-Temperature MOVPE-Regrown Ohmic Contacts

Arkka Bhattacharyya¹, Saurav Roy¹, Praneeth Ranga¹, Daniel Shoemaker², Yiwen Song², James Spencer Lundh², Sukwon Choi², and Sriram Krishnamoorthy^{1*}

Abstract— We report on the demonstration of metal-organic vapor phase epitaxy-regrown (MOVPE) ohmic contacts in an all MOVPE-grown β -Ga₂O₃ metal-semiconductor field effect transistor (MESFET). The low-temperature (600°C) heavy (n⁺) Si-doped regrown layers exhibit extremely high conductivity with sheet resistance of 73 Ω /sq and a record metal/n⁺-Ga₂O₃ contact resistance of 0.08 Ω .mm and specific contact resistivity of 8.3×10^{-7} Ω .cm² were achieved. The fabricated MESFETs exhibit a maximum drain-to-source current of 130 mA/mm, a high I_{ON}/I_{OFF} of $> 10^{10}$ with a high power FOM of 25 MW/cm² was achieved without any field plates. Nanoparticle-assisted Raman thermometry, thermal modeling, and infrared thermography were performed to assess the device self-heating under the high current and power conditions. This demonstration shows the promise of MOVPE technique for realization of high performance lateral β -Ga₂O₃ devices and also highlights the need for device-level thermal management.

Index Terms— Ga₂O₃, MOVPE, contact resistance, ohmic contact, regrowth, power switch, MESFET, self-heating, thermal modeling, infrared thermography.

I. INTRODUCTION

β -Ga₂O₃, being an ultra-wide bandgap material ($E_g = 4.6 - 4.9$ eV), has a projected performance advantage over other predominant wide bandgap semiconductors such as SiC and GaN [1], [2]. With an added advantage of potentially being cost-effective due to the availability of large-area melt-grown bulk substrates, it has the potential to be the material of choice for next generation solid state power switching applications. Demonstration of β -Ga₂O₃-based lateral field-effect transistors with average breakdown fields of up to 4 MV/cm and breakdown voltages of 8 kV not only strengthens this promise but also demonstrates the rapid progress and breakthroughs achieved in β -Ga₂O₃-based device design and device processing technologies [3]–[5]. Further advancement of

material and device engineering and processing is critical to achieving high breakdown voltage and low ON resistance with high ON current simultaneously.

Low resistance ohmic contact is an essential part of a lateral device, apart from high mobility channel layers, to realize high performance β -Ga₂O₃ based transistors with high current densities and lower conduction losses. To avoid gate-recessing, various techniques such as Si-ion implantation, spin-on-glass (SOG), regrown contact layers using molecular-beam epitaxy (MBE) and pulsed-laser deposition (PLD) have been developed to realize source/drain (S/D) ohmic contacts in Ga₂O₃-based MOSFETs and MESFETs [6]–[10]. While regrown contacts have reportedly provided the lowest contact resistances, the Ga₂O₃ devices in literature which have used regrown S/D contacts have so far mostly relied on the MBE technique to regrow the heavily-doped n⁺ regions [9]. Metalorganic vapor phase epitaxy (MOVPE) as an epitaxial growth technique has the advantage of growing β -Ga₂O₃ homoepitaxial films with high room-temperature electron mobility values (close to the theoretical limit) and could be promising for fabricating Ga₂O₃ lateral FETs with high current densities [11]–[14]. In this work, we demonstrate for the first time, using selective area epitaxy approach, realization of low resistance regrown S/D contacts in a fully MOVPE-grown Ga₂O₃ lateral MESFET with high current densities and comparatively high average electric-field (without field plates or passivation).

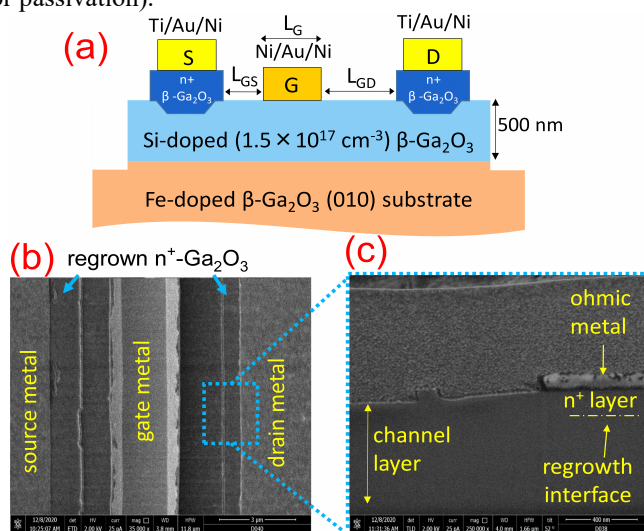


Fig 1: (a) Schematic of the fully MOVPE-grown Ga₂O₃ MESFET with regrown ohmic contacts (b) Top view SEM image of the MESFET

¹ A. Bhattacharyya, S. Roy, P. Ranga and S. Krishnamoorthy are with the Department of Electrical and Computer Engineering, University of Utah, Salt Lake City, Utah, USA 84112 (e-mail: sriram.krishnamoorthy@utah.edu).

D. Shoemaker, Y. Song, J. S. Lundh and S. Choi are with the Department of Mechanical Engineering, The Pennsylvania State University, University Park, Pennsylvania, 16802, USA (e-mail: sukwon.choi@psu.edu).

* Corresponding author e-mail: sriram.krishnamoorthy@utah.edu

showing the regrown access regions (c) cross-sectional SEM of the contact region showing the estimated regrowth interface.

II. DEVICE GROWTH AND FABRICATION

The epitaxial structure shown in Fig. 1(a) was grown using an Agnition Agilis MOVPE reactor. A 500 nm thick lightly Si-doped ($1.5 \times 10^{17} \text{ cm}^{-3}$) β -Ga₂O₃ channel was grown on a (010) Fe-doped semi-insulating Ga₂O₃ substrate (NCT Japan) at a temperature of 810°C using triethylgallium, O₂ and silane gases as precursors and Ar as the carrier gas. Prior to loading into the growth reactor, the substrate was dipped in a diluted HF solution for 30 mins. From Hall measurements, the channel charge and mobility were measured to be $5.7 \times 10^{12} \text{ cm}^{-2}$ and $132 \text{ cm}^2/\text{Vs}$ respectively giving a channel sheet resistance $R_{\text{sh,ch}} = 8.2 \text{ k}\Omega/\square$.

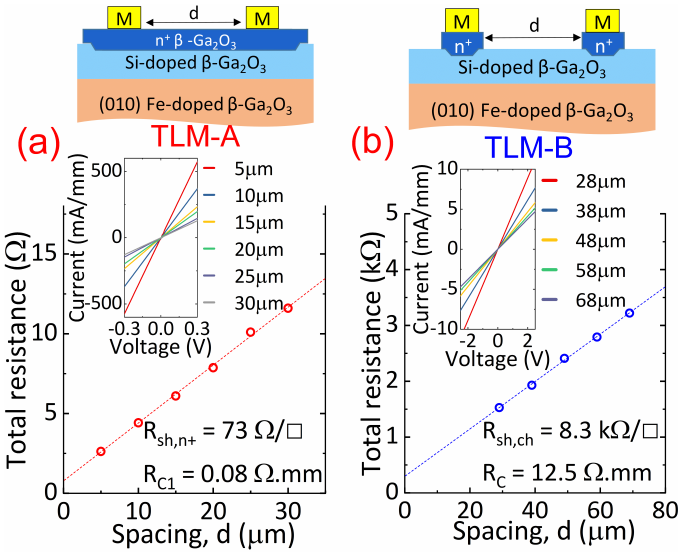


Fig 2: Schematic of TLM structure, corresponding IV plots (inset) and total resistance vs contact spacing plots of (a) TLM pads on the MOVPE-regrown n^+ Ga₂O₃ region and (b) TLM pads with patterned MOVPE-regrown n^+ ohmic contacts.

The device mesa isolation was performed using a Ni/SiO₂ hard mask and SF₆/Ar plasma chemistry based ICP-RIE dry etching all the way to the substrate. A selective area MOVPE regrowth process was developed to obtain low-resistance S/D ohmic contacts. First, a sacrificial 500 nm thick SiO₂ layer was blanket-deposited using plasma-enhanced chemical vapor deposition. The S/D contact regions were then defined using a Ni layer patterned by photolithography and lift-off. Using Ni as the hard mask, the SiO₂ in the S/D contact regions was removed by the same SF₆/Ar plasma based directional ICP-RIE dry etching (150W RF and 600W ICP). The etching in the contact regions was extended down to the Ga₂O₃ layer with an estimated Ga₂O₃ trench depths of 10-20 nm. The Ni mask was then selectively removed by dipping the sample in a diluted aqua regia solution. Next, heavily Si-doped ($2 \times 10^{20} \text{ cm}^{-3}$) Ga₂O₃ was grown in the open S/D regions using MOVPE at a lowered growth temperature of 600°C. The 120 nm thick n^+ -Ga₂O₃ growth step was preceded by a heavy Si delta doping at

the etched Ga₂O₃ surface in the contact region [15], [16]. The heavy Si delta doping was done at the etched surface to suppress any epilayer/regrown interface depletion due to any F⁻ ion incorporation caused by the SF₆ dry etching. Following the regrowth step, the polycrystalline Ga₂O₃ layer in the regions outside the contact area was removed by dissolving the sacrificial SiO₂ in an HF solution. Ohmic metal stack Ti/Au/Ni (20nm/100nm/30nm) was evaporated on the regrown contact regions by photolithography patterning and lift off followed by a 470°C anneal in N₂ for 1.5 mins. Finally, a Ni/Au/Ni (30nm/100nm/30nm) metal stack was evaporated to form the Schottky gate for the MESFET structure.

III. RESULTS AND DISCUSSIONS

Fig.1(b) shows the top-view SEM image of the MESFET structure. The regrown layers were indistinguishable from the channel region and the surface morphology was similar to that of the channel. From the cross-sectional SEM (Fig.1(c)) image, no crevices or cracks were visible between the channel and the regrown region. The regrown n^+ -Ga₂O₃/channel interface was very conformal with no visible interface as expected from the MOVPE growth technique.

For an uniformly doped Ga₂O₃ channel with n^+ -Ga₂O₃ contacts, the total contact resistance (R_C) consists of three components: 1) R_{C1} = metal/ n^+ regrown Ga₂O₃ interface contact resistance, 2) R_{n^+} = resistance of the regrown n^+ -Ga₂O₃ access region and 3) R_{C2} = n^+ regrown Ga₂O₃/lightly doped Ga₂O₃ channel interface resistance. From TLM A (metal contact pads spaced out on the isolated regrown n^+ -Ga₂O₃ slab), sheet resistance of the regrown region (R_{sh,n^+}) is extracted to be $73 \text{ }\Omega/\square$. A record low metal/ n^+ -Ga₂O₃ interface contact resistance (R_{C1}) of $0.08 \text{ }\Omega.\text{mm}$ and specific contact resistance (ρ_{C1}) of $8.3 \times 10^{-7} \text{ }\Omega.\text{cm}^2$ were achieved. This shows the low-temperature MOVPE-regrown Ga₂O₃ was of high quality and highly conducting. From TLM-B structure (Fig.2(b)), $R_{\text{sh,ch}}$ and total contact resistance R_C are extracted to be $8.3 \text{ k}\Omega/\square$ and $12.5 \text{ }\Omega.\text{mm}$, respectively. R_{n^+} is estimated from the regrown Ga₂O₃ access region dimensions to be $0.2 \text{ }\Omega.\text{mm}$ [17] giving R_{C2} a value of $12.2 \text{ }\Omega.\text{mm}$. This shows the total contact resistance is mainly limited by R_{C2} . As this is a lightly doped channel, this could be due to the etch damage at the regrowth interface caused by the F-based dry etch and could be improved by switching over to a BCl₃ – based dry etching. However, it is to be noted that $R_{\text{sh,ch}}$ from TLM after the regrowth process matches with that of Hall measurements done before the regrowth indicating our low-temperature regrowth process has no detrimental effect on the active region material quality.

Representative DC device output ($I_{\text{DS}}-V_{\text{DS}}$) and transfer ($I_{\text{DS}}-V_{\text{GS}}$) curves of the fully MOVPE-grown Ga₂O₃ MESFET is shown in Fig. 3(a,b) with a device dimension of $L_{\text{GS}}/L_{\text{G}}/L_{\text{GD}} = 1\mu\text{m}/1.7\mu\text{m}/1.6\mu\text{m}$. The maximum normalized drain-to-source current ($I_{\text{DS,MAX}}$) was recorded to be 130mA/mm at zero gate bias and a drain bias of 15 V. The device exhibits a subthreshold slope of 122 mV/dec and a very large $I_{\text{ON}}/I_{\text{OFF}}$ ratio of $>10^{10}$ with the OFF-state current mainly limited by the measurement tool detection limit (below noise floor). From

the transfer curve, the threshold voltage of -25V and a max transconductance of 4.8 mS/mm (at $V_{GS} = -15\text{V}$) were extracted. It is to be noted that our MESFET exhibits a high ON current (130 mA/mm) without even operating at a positive V_{GS} and an extremely low leakage ($<10^{-12}\text{ A/mm}$) simultaneously, thus, giving our depletion-mode (D-mode) $\beta\text{-Ga}_2\text{O}_3$ channel MESFET one of the highest I_{ON}/I_{OFF} ratio in its class. This was achieved by the proper substrate preparation to suppress the parasitic channel at the epilayer/substrate interface, maintaining a high-quality of the MOVPE-grown channel layer on the modified substrate and low-temperature device processing (low-temperature MOVPE contact regrowth) that preserved the high-mobility of carriers in the active region. Using TLM and CV measurements post processing, the effective drift mobility of carriers in the channel region was estimated to be $\sim 130\text{ cm}^2/\text{Vs}$ for $V_{GS}=0\text{V}$. Further improvement in the maximum ON currents and device performance can be achieved by realizing an accumulation channel (positive gate bias) by adopting a MOSFET structure and higher channel length to thickness ratio (higher channel aspect ratio) for improved gate control.

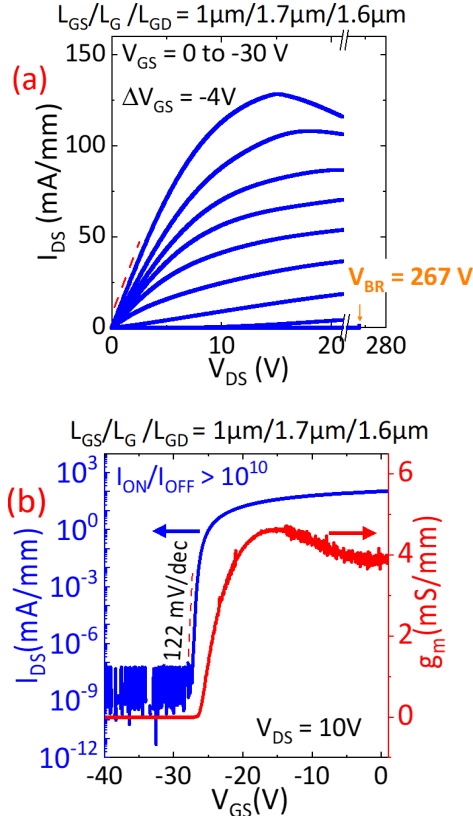


Fig 3: (a) Output characteristics (b) Transfer characteristics of the fully MOVPE $\beta\text{-Ga}_2\text{O}_3$ MESFET with regrown S/D contacts.

Three-terminal OFF state breakdown measurements were performed in Fluorinert solution at V_{GS} of -30V . A breakdown voltage (V_{BR}) of 267V was extracted for a device with L_{GD} of $1.6\mu\text{m}$. Using a 2D Sentaurus TCAD simulation of the actual structure, the peak and average breakdown fields were estimated to be $7 \times 10^6\text{ MV/cm}$ and $1.9 \times 10^6\text{ MV/cm}$

respectively for this device with L_{GD} of $1.6\mu\text{m}$. With a calculated specific ON resistance of $3.7\text{ m}\Omega\cdot\text{cm}^2$, the power figure of merit is estimated to be 19 MW/cm^2 . By increasing L_{GD} , the maximum V_{BR} measured is 778V for $L_{GD}=20\mu\text{m}$. Figure 4(b) shows the $I_{DS,MAX}$ and V_{BR} as a function of L_{GD} in these devices. The maximum FOM of 25 MW/cm^2 was achieved for a device with L_{GD} of $5\mu\text{m}$. This FOM value is higher than most of the D-mode $\beta\text{-Ga}_2\text{O}_3$ channel MESFETs which do not implement any field-management or passivation techniques.

Absolute $I_{DS,MAX}$ values are measured in devices with smaller channel widths (schematic in Fig.4(a) inset) that led to devices with different channel width to length ratio (W/L) across the same wafer keeping all other device dimensions ($L_{GS}/L_G/L_{SD} = 2.8\mu\text{m}/2.1\mu\text{m}/8.4\mu\text{m}$) the same. For these long channel devices, the absolute $I_{DS,MAX}$ values scaled linearly with W/L as shown in Fig.4(a). The normalized $I_{D,MAX}$ values remain constant throughout the W/L ratio. This indicates the $I_{DS,MAX}$ values in these devices are not limited by contact resistance of the S/D ohmic contacts. In fact, the $I_{DS,MAX}$ values were limited due to self-heating in these devices evident from the reduction of I_{DS} value at higher V_{DS} values as seen in Fig.3(a) [18], [19].

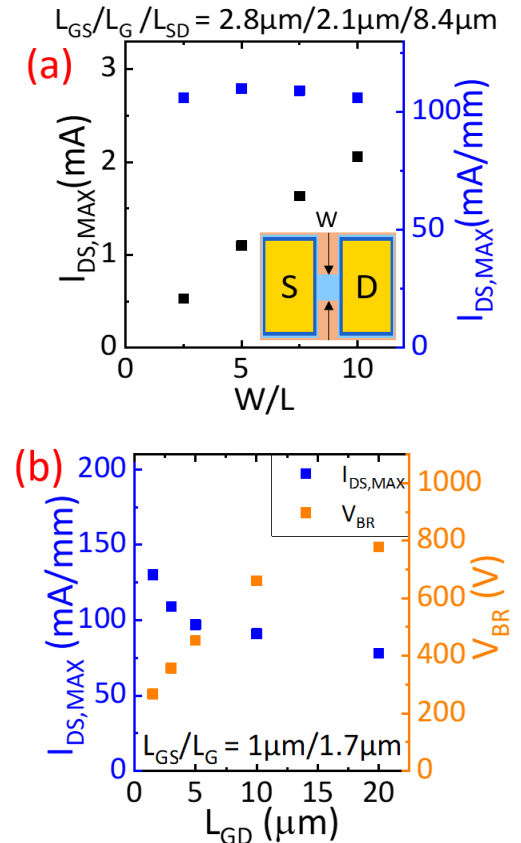


Fig 4: (a) $I_{DS,MAX}$ for devices with different channel width to length ratios (W/L) (b) $I_{DS,MAX}$ and V_{BR} of devices with different L_{GD} .

To estimate the channel temperature at which self-heating induced current droop occurs in Fig. 3 (a) ($V_{GS}=0\text{V}$, $V_{DS}=15\text{V}$, $P=0.96\text{ W/mm}$), the device was characterized via

nanoparticle-assisted Raman thermometry using a Horiba LabRAM HR Evolution spectrometer. The temperature was measured by monitoring the E_g mode frequency shift of an anatase TiO_2 nanoparticle deposited near the drain side corner of the gate [20]. Experimental results were validated using a three-dimensional finite element thermal model. Details of the thermal modeling procedure can be found in Ref.[20], [21]. At the current inflection point in Fig. 3(a) ($P = 0.96 \text{ W/mm}$), the estimated channel temperature was $\sim 81^\circ\text{C}$. To visualize the device self-heating under high power conditions, infrared (IR) thermal microscopy was performed using a QFI medium wavelength infrared (MWIR) InfraScope with a 15x objective [22]. Results of the thermal analysis are illustrated in Fig. 5.

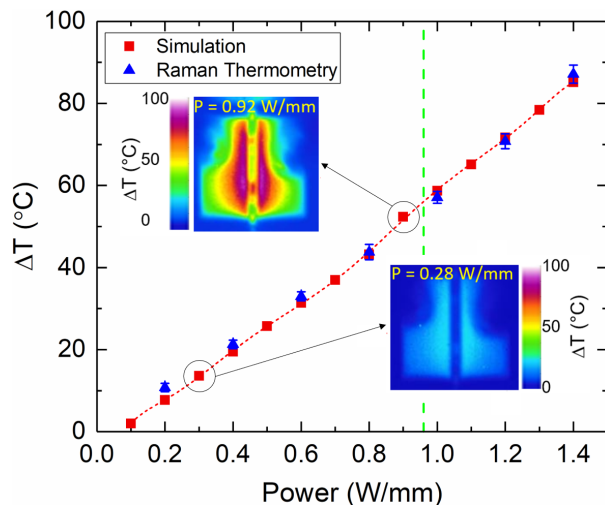


Fig 5: The channel temperature rise determined by Raman thermometry, thermal modeling, and IR thermography. The green dashed line corresponds to the current inflection point in Fig. 3(a).

IV. CONCLUSION

We demonstrate the use of MOVPE technique to realize low-resistance regrown ohmic contacts in a fully MOVPE-grown lateral $\beta\text{-Ga}_2\text{O}_3$ MESFET. The low-temperature (600°C) heavy (n^+) Si-doped regrown layers exhibit extremely high conductivity with sheet resistance of $73 \Omega/\text{sq}$ and a record metal/ $n^+\text{-Ga}_2\text{O}_3$ contact resistance of $0.08 \Omega\cdot\text{mm}$ and specific contact resistivity of $8.3 \times 10^{-7} \Omega\cdot\text{cm}^2$ were achieved. The MESFET shows a maximum current density of 130 mA/mm at zero gate bias and an extremely low leakage current ($<10^{-12} \text{ A/mm}$). Average breakdown field and maximum FOM of 1.9 MV/cm and 25 MW/cm^2 respectively are achieved even without field-plates or passivation. However, it should be noted that the enabled high current/power capabilities must be supported by effective thermal management solutions [22]. This demonstration of first-generation fully MOVPE-grown $\beta\text{-Ga}_2\text{O}_3$ FETs shows the potential of MOVPE technique for realizing high ON currents in $\beta\text{-Ga}_2\text{O}_3$ -based devices as well as a promising technique for low-temperature Ohmic contact regrowth. Further improvement in device performance can be achieved by implementing field-management techniques in a MOSFET structure along with channel engineering.

ACKNOWLEDGMENT.

This work was supported by II–VI foundation Block Gift Program. We also thank the Air Force Office of Scientific Research under Award No. FA9550-18-1-0507 (Program Manager: Dr. Ali Sayir) for financial support. Funding for Penn State was provided by the AFOSR Young Investigator Program (Grant No. FA9550-17-1-0141, Program Officers: Dr. Brett Pokines and Dr. Michael Kendra, also monitored by Dr. Kenneth Goretta) and NSF (CBET-1934482, Program Manager: Dr. Ying Sun).

REFERENCES

- [1] M. Higashiwaki and G. H. Jessen, "Guest Editorial: The dawn of gallium oxide microelectronics," *Appl. Phys. Lett.*, vol. 112, no. 6, p. 060401, Feb. 2018, doi: 10.1063/1.5017845.
- [2] M. Higashiwaki, K. Sasaki, A. Kuramata, T. Masui, and S. Yamakoshi, "Gallium oxide (Ga_2O_3) metal-semiconductor field-effect transistors on single-crystal $\beta\text{-Ga}_2\text{O}_3$ (010) substrates," *Appl. Phys. Lett.*, vol. 100, no. 1, p. 013504, Jan. 2012, doi: 10.1063/1.3674287.
- [3] N. K. Kalarickal *et al.*, "Electrostatic Engineering using Extreme Permittivity Materials for Ultra-wide Bandgap Semiconductor Transistors," Jun. 2020, Accessed: Jan. 09, 2021. [Online]. Available: <https://arxiv.org/abs/2006.02349v1>.
- [4] S. Sharma, K. Zeng, S. Saha, and U. Singiseti, "Field-Plated Lateral Ga_2O_3 MOSFETs With Polymer Passivation and 8.03 kV Breakdown Voltage," *IEEE Electron Device Lett.*, vol. 41, no. 6, pp. 836–839, Jun. 2020, doi: 10.1109/LED.2020.2991146.
- [5] A. J. Green *et al.*, "3.8-MV/cm Breakdown Strength of MOVPE-Grown Sn-Doped $\beta\text{-Ga}_2\text{O}_3$ MOSFETs," *IEEE Electron Device Lett.*, vol. 37, no. 7, pp. 902–905, Jul. 2016, doi: 10.1109/LED.2016.2568139.
- [6] K. Sasaki, M. Higashiwaki, A. Kuramata, T. Masui, and S. Yamakoshi, "Si-Ion Implantation Doping in $\beta\text{-Ga}_2\text{O}_3$ and Its Application to Fabrication of Low-Resistance Ohmic Contacts," *Appl. Phys. Express*, vol. 6, no. 8, p. 086502, Jul. 2013, doi: 10.7567/APEX.6.086502.
- [7] K. Zeng *et al.*, "Ga $_2$ O $_3$ MOSFETs Using Spin-On-Glass Source/Drain Doping Technology," *IEEE Electron Device Lett.*, vol. 38, no. 4, pp. 513–516, Apr. 2017, doi: 10.1109/LED.2017.2675544.
- [8] K. D. Chabak *et al.*, "Lateral $\beta\text{-Ga}_2\text{O}_3$ field effect transistors," *Semicond. Sci. Technol.*, vol. 35, no. 1, p. 013002, Nov. 2019, doi: 10.1088/1361-6641/ab55fe.
- [9] Z. Xia *et al.*, "Delta Doped $\beta\text{-Ga}_2\text{O}_3$ Field Effect Transistors With Regrown Ohmic Contacts," *IEEE Electron Device Lett.*, vol. 39, no. 4, pp. 568–571, Apr. 2018, doi: 10.1109/LED.2018.2805785.
- [10] M. H. Wong, Y. Nakata, A. Kuramata, S. Yamakoshi, and M. Higashiwaki, "Enhancement-mode Ga $_2$ O $_3$ MOSFETs with Si-ion-implanted source and drain," *Appl. Phys. Express*, vol. 10, no. 4, p. 041101, Mar. 2017, doi: 10.7567/APEX.10.041101.
- [11] "Low temperature homoepitaxy of (010) $\beta\text{-Ga}_2\text{O}_3$ by metalorganic vapor phase epitaxy: Expanding the growth window: Applied Physics Letters: Vol 117, No 14." <https://aip.scitation.org/doi/full/10.1063/5.0023778> (accessed Oct. 29, 2020).
- [12] Z. Feng, A. F. M. Anhar Uddin Bhuiyan, M. R. Karim, and H. Zhao, "MOCVD homoepitaxy of Si-doped (010) $\beta\text{-Ga}_2\text{O}_3$ thin films with superior transport properties," *Appl. Phys. Lett.*, vol. 114, no. 25, p. 250601, Jun. 2019, doi: 10.1063/1.5109678.
- [13] Y. Zhang *et al.*, "MOCVD grown epitaxial $\beta\text{-Ga}_2\text{O}_3$ thin film with an electron mobility of $176 \text{ cm}^2/\text{V}\cdot\text{s}$ at room temperature," *APL Mater.*, vol. 7, no. 2, p. 022506, Dec. 2018, doi: 10.1063/1.5058059.
- [14] G. Seryogin *et al.*, "MOCVD growth of high purity Ga $_2$ O $_3$ epitaxial films using trimethylgallium precursor," *Appl. Phys. Lett.*, vol. 117, no. 26, p. 262101, Dec. 2020, doi: 10.1063/5.0031484.
- [15] P. Ranga *et al.*, "Delta-doped $\beta\text{-Ga}_2\text{O}_3$ thin films and $\beta\text{-Ga}_2\text{O}_3$ -(Al $_0.26$ Ga $_0.74$) $_2$ O $_3/\beta\text{-Ga}_2\text{O}_3$ heterostructures grown by

- metalorganic vapor-phase epitaxy,” *Appl. Phys. Express*, vol. 12, no. 11, p. 111004, Nov. 2019, doi: 10.7567/1882-0786/ab47b8.
- [16] P. Ranga, A. Bhattacharyya, A. Chmielewski, S. Roy, N. Alem, and S. Krishnamoorthy, “Delta-doped β -Ga₂O₃ films with narrow FWHM grown by metalorganic vapor-phase epitaxy,” *Appl. Phys. Lett.*, vol. 117, no. 17, p. 172105, Oct. 2020, doi: 10.1063/5.0027827.
- [17] J. Guo *et al.*, “MBE-Regrown Ohmics in InAlN HEMTs With a Regrowth Interface Resistance of 0.05 $\Omega \cdot \text{cm}$,” *IEEE Electron Device Lett.*, vol. 33, no. 4, pp. 525–527, Apr. 2012, doi: 10.1109/LED.2012.2186116.
- [18] “Depletion-mode Ga₂O₃ metal-oxide-semiconductor field-effect transistors on β -Ga₂O₃ (010) substrates and temperature dependence of their device characteristics: Applied Physics Letters: Vol 103, No 12.” <https://aip.scitation.org/doi/full/10.1063/1.4821858> (accessed Jan. 09, 2021).
- [19] N. A. Blumenschein *et al.*, “Self-Heating Characterization of β -Ga₂O₃ Thin-Channel MOSFETs by Pulsed $SIS - SV$ and Raman Nanothermography,” *IEEE Trans. Electron Devices*, vol. 67, no. 1, pp. 204–211, Jan. 2020, doi: 10.1109/TED.2019.2951502.
- [20] J. S. Lundh *et al.*, “Multidimensional thermal analysis of an ultrawide bandgap AlGa_N channel high electron mobility transistor,” *Appl. Phys. Lett.*, vol. 115, no. 15, p. 153503, Oct. 2019, doi: 10.1063/1.5115013.
- [21] B. Chatterjee *et al.*, “Electro-thermal co-design of β -(Al_xGa_{1-x})₂O₃/Ga₂O₃ modulation doped field effect transistors,” *Appl. Phys. Lett.*, vol. 117, no. 15, p. 153501, Oct. 2020, doi: 10.1063/5.0021275.
- [22] J. Dallas *et al.*, “Thermal characterization of gallium nitride p-i-n diodes,” *Appl. Phys. Lett.*, vol. 112, no. 7, p. 073503, Feb. 2018, doi: 10.1063/1.5006796.
- [23] B. Chatterjee, K. Zeng, C. D. Nordquist, U. Singiseti, and S. Choi, “Device-Level Thermal Management of Gallium Oxide Field-Effect Transistors,” *IEEE Trans. Compon. Packag. Manuf. Technol.*, vol. 9, no. 12, pp. 2352–2365, Dec. 2019, doi: 10.1109/TCPMT.2019.2923356